Chinese Journal of Polymer Science Vol. 33, No. 10, (2015), 1477−1490

Chinese Journal of Polymer Science
© Chinese Chemical Society
Institute of Chemistry, CAS
Springer-Verlag Berlin Heidelberg 2015

The Toughening Behavior of the PP/POE Alternating Multilayered Blends under EWF and Impact Tensile Methods*

Chun-hai Li, Jian-feng Wang, Ji-wei Guo, Hong Wu** and Shao-yun Guo**
The State Key Laboratory of Polymer Materials Engineering, Polymer Research Institute of Sichuan University, Chengdu 610065, China

Abstract The multilayered polypropylene (PP) and poly(ethylene-*co*-octene) (POE) sheets were prepared by the micro-layered co-extrusion system. The essential work of fracture (EWF) and the impact tensile methods have been successfully used to evaluate the toughening behaviors of the PP/POE multilayered blends under quasi-static and dynamic uniaxial tensile stress, respectively. The experimental results indicate that the multilayered structure plays a key role in the toughening behaviors. On increasing the layer number of the multilayered blends, the specific essential work of fracture, w_e, increases obviously. As for the βw_p, there is no obvious variation in the multilayered blends with low POE content (6.79%), however, obvious enhancement is observed with increasing the layer number of the high POE content multilayered blends (16.57%). Compared with the conventional blends, the multilayered blends with 6.79% POE content are effective to increase the value of w_e. Additionally, the multilayered blends with high layer numbers present absolute advantage in improving the impact tensile values.

Keywords: Multilayer; EWF; Impact tensile; PP; POE.

INTRODUCTION

Polypropylene (PP), an important commodity plastic with many excellent properties, has been widely used in the construction, automobile and household appliance industries. However, the application of PP is greatly limited by its low impact strength. To overcome this disadvantage, various methods have been used to improve its impact strength. One of the most effective methods is blending PP with the elastomer POE and many research results have demonstrated that the shape, sizes and the distribution of the POE impact the materials toughness greatly[1−5].

Fu *et al.*[1] controlled the hierarchical structure of PP/POE systems through dynamic packing injection technology, and obtained the samples with highly oriented PP matrix and elongated POE particles. Most interestingly, the elongated POE particles could not improve the impact toughness of the PP/POE system. By controlling the interfacial interaction and the viscosity ratio of elastomers domain to the PP matrix, Zhang *et al.*[2, 3] achieved the POE dispersing phase with the spherical, elliptical, rod-like and even the fibrillar morphology. They found that the toughness of the blends with soft fibrillar morphology was lower compared to that with spherical, elliptical, and even the rod-like morphology. Paul *et al.*[4] found that the addition of the clay can reduce the sizes of the POE particles and finally facilitated the blends with high toughness. Wang *et al.*[5]

* This work was financially supported by the National Natural Science Foundation of China (Nos. 51273132, 51227802 and 51121001) and Program for New Century Excellent Talents in Universities (No. NCET-13-0392).
** Corresponding authors: Hong Wu (吴宏), E-mail: wh@scu.edu.cn
Shao-yun Guo (郭少云), E-mail: sguo@scu.edu.cn
Received April 17, 2015; Revised June 22, 2015; Accepted June 30, 2015
doi: 10.1007/s10118-015-1692-1

fabricated the alternating multilayered blends by alternating the PP and PP/POE blends through micro-layered co-extrusion technology, in detail, the POE particles were alternately distributed in the PP matrix. Most interestingly, compared with the random distribution of POE particles, the unique alternating distribution of POE particles endows the multilayered blends with great toughness at –40 °C. Just as the aforementioned description, many researches have been done to investigate the influences of the shape, sizes and distribution of the POE dispersing phase on the toughness of the PP/POE system. Actually, the damage readily occurs at the weak interfaces, and then the large and continuous interfaces are great advantage in accumulating micro-cracks and delaminations, which are crucial to toughen the materials[6–9]. Therefore, several advanced technologies, such as layer-by-layer[10], electrical fields[11] tape-casting[12] and gel casting combined with hot-pressing[13, 14] have been developed for preparing novel materials with tremendous and continuous weak interfaces. However, these approaches are always limited to fabricating thin films and/or require multiple processing steps[15]. Fortunately, in past decades, micro-layered co-extrusion technology[16] was developed as a novel technology in polymer melt processing to tune the material properties, such as electrical[17], flame resistance[18], barrier[19], optical[20], and especially mechanical properties[9, 21–23]. Hence, in our previous work, by using the micro-layered co-extrusion technology, the alternating multilayered PP/POE system was fabricated, indicating amounts of weak and continuous interfaces were introduced. In our opinion, the notable improvement of Izod impact strength of the multilayered blends was ascribed to the synergetic effects of the interfaces delaminations, craze deflection and a larger subcritical damage zone (stress whitening zone)[9]. However, to our best knowledge, the impact test is an empirical method and the toughness obtained by that way depends on the specimen sizes and testing conditions, which can not represent the truth toughness of a given material. Inversely, the inherent toughness of a given material can be determined by adapting the fracture mechanics. Owing to the simplicity of the experimental process and data manipulation of the essential work of fracture measurement (EWF), the EWF recently has gained more and more attentions and acceptances for determining the inherent toughness of various ductile polymeric materials, especially for samples in the form of films or thin sheets[24]. Although the toughening behaviors of PP/POE systems have been widely evaluated through the EWF method[25, 26], its application to multilayered polymeric films, where the POE phase is distributed with a laminar morphology is still not reported.

Just as the above discussion, the laminar morphology of the POE indicates large and continuous interfaces, which are crucial to toughen materials. Therefore, in order to further evaluate the toughening behavior of the PP/POE alternating multilayered blends, in this present work, the EWF approach is used to evaluate the toughening behaviors under quasi-static uniaxil tensile stress, whereas the impact tensile is used to evaluate the toughening behaviors under dynamical stress.

THEORY

The EWF method, first proposed by Cotterell and Reddell[27], is based on Broberg's work on stable crack growth[28], and then has been developed by Karger-Kocsis[29, 30] and Mai[31]. According to energy partition[32], the total fracture work (W_f) used to fracture a pre-cracked specimen can be consumed in two distinct zone, the inner and outer zones (as depicted in Fig. 1). The inner zone, also called the process zone, is where the real fracture process takes place with the formation of new surfaces. The energy associated with it, the essential work of fracture (W_e) is proportional to the ligament section, $l \cdot t$. In the outer zone, called also the plastic zone, the energy involved is the non-essential work of fracture or plastic work (W_p), which is employed basically in plastic deformation and other dissipative process. The work consumed in this zone is proportional to the volume of the deformed region. Base on the above concept, the following expressions can be followed:

$$W_f = W_e + W_p = w_f l \cdot t = w_e l \cdot t + w_p \beta l^2 \cdot t$$

which can be written as:

$$w_f = w_e + \beta w_p l$$

where w_f is the specific fracture work, l is the ligament length, t is the thickness of specimen, β is a shape factor that is associated with the dimension of the plastic zone and w_e and w_p are the specific essential work of fracture and specific non-essential work of fracture or specific plastic work, respectively. The specific essential work of fracture, w_e has been shown to be a material property and relate to the inner fracture morphology[33]. While, the specific plastic deformation work of fracture, w_p, is not a material constant and depends on the shape of the plastic zone, the specimen geometry, testing speed, *etc*[34]. In addition, the βw_p term provides a highly morphology-sensitive parameter, which is very useful for evaluation of toughness in thin specimens. w_e and βw_p are determined by a linear interpolation of a series of experimental data of w_f obtained by testing specimens having different ligament lengths[35, 36].

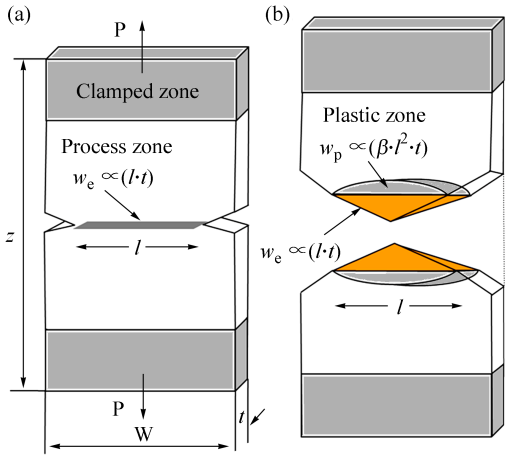


Fig. 1 The deeply double edge notched tension specimen (DDENT) used in the EWF test: (a) before the EWF test and (b) after the EWF test

EXPERIMENTAL

Materials

Polypropylene is of grade 1300 with a MFI of 2.0 g/10 min at 230 °C, 2.16 kg, supplied by Mao Ming Petro-chemistry Co. POE is Engage 8100 manufactured by Dow Chemical, with an octane-comonomer molar content of 9.8% and a MFI of 1.0 g/10 min, at 190 °C, 2.16 kg. The densities of them are 0.9029 and 0.8785 g/cm^3 (measured by MatsuHaku, GH-120M), respectively.

Samples Preparation

Multilayered sheets consisting of alternating PP and POE layers were extruded with a multilayered co-extrusion system developed by our laboratory, as described previously[5, 9]. The 8-, 32- and 128-layer specimens were extruded by the variation of the number of LMEs. In comparison, the neat PP samples were also prepared under the same shearing force history through one of extruders of the multilayered co-extrusion system. All of the multilayered sheets were about 1.3 mm thick and 30 mm wide after cooling. Two POE volume contents multilayered sheets were produced through controlling the feeding ratio. In the processing, the extruder temperature was 160-180-190-200-200 °C for the PP section and 90-180-190-200-200 °C for POE section, respectively. In comparison, conventional PP/POE blending samples were prepared by mixing equal mass fraction of 8-, 32- and 128-layer samples. The mixing condition was 30 r/min at 200 °C for 8 min. In order to remove the effects of orientation and crystalline differences on the mechanical properties, all samples before testing were thermally treated under 10 MPa for 10 min at 200 °C. For the EWF test specimens, after the thermal treatment, the thickness of the samples decreases down to 1 mm while the width increases to about 40 mm.

Polarized Optical Microscopy (POM)

To examine the multilayered structure morphologies of the different layered samples, a rotary microtome (YD-2508B) was used to cut a 20 μm slice from the co-extrusion multilayered sheets along the transverse direction. The sample slice was placed between two glass slices and then inspected on a polarized optical microscope (POM, Leica, DM2500P).

Essential Work of Fracture Measurements (EWF)

The DDENT specimens (length × width × thickness = 100 mm × 35 mm × 1 mm), as seen in Fig. 1 were cut from the thermal treatment specimens along the extrusion direction. As for conventional blends, the blends were first hot-compressed into 10 mm × 10 mm × 1 mm and then cut according the Fig. 1. The sharp pre-cracks on both sides of the specimens were made perpendicular to the tensile direction with a fresh razor blade. To meet the plane stress condition of the specimens, their ligament range was limited $3t < l < w/3$[37].

The EWF tests of the DDENT specimens were performed using an Instron5567 tension machine (Canton, MA, USA) with a 1000 N load cell at a room temperature of 23 °C. The crosshead speed was set at 10 mm/min. The tensile is carried out along the extrusion direction, the load displacement curves were recorded, and the energy that was absorbed until failure was calculated by the computer integration of the load displacement curves. For each material, nearly 16 specimens were tested with different ligament lengths. Before the EWF testing, the ligament lengths and the thickness of all the specimens were measured using a microscope and a vernier caliper, respectively.

No-notched Impact Tensile Test

As is shown in Fig. 2, the testing geometry was cut along the extrusion direction from the centre of the thermal treatment samples, as for conventional blends, the blends were first hot-compressed into 10 mm × 10 mm × 1.3 mm and then cut according the Fig 2. Impact tensile of the samples was performed along the extrusion direction by an XJ-50 (JJ-TEST, China) impact pendulum machine, according to the GB/T13525. The impact velocity was 3.8 m/s. The impact energy was 15 J. Testing was carried out at ambient temperature (23 °C). Each impact test included at least 8 parallel experiments, and the results were averaged.

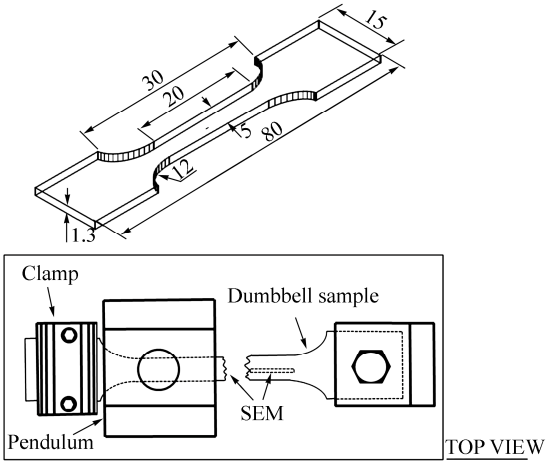


Fig. 2 Schematic representation of impact tensile test (The testing is along the extrusion direction.)

Scanning Electron Microscopy (SEM)

To observe the morphologies of the inner fracture process zone after the EWF test, the fracture specimens were cryofractured in liquid nitrogen, after which the fracture morphologies were examined by SEM (JSM-5900LV, Japan). Besides, the fracture surface morphologies and the bulk morphologies (beneath the fracture surface) of the impact tensile samples were also examined by the SEM. In order to examine the bulk morphologies, the impacted samples were cryogenically polished along the impact tensile direction but perpendicular to the layer

plane with a tungsten knife at −110 °C through the Leica RM2265 microtome (as shown in Fig. 2). Before SEM characterization, all the surfaces were sputter-coated with a gold layer.

Measurement of the Density and Layer Thickness

The average thickness of each PP or POE layer was calculated by averaging the individual PP or POE layer thickness of the co-extrusion sheets, which was obtained by measuring the POM micrographs of the multilayered samples with the Image-Pro-Plus soft. Table 1 shows the sample code, total sheet thickness, average PP or POE layer thickness, and the POE volume content in the multilayered and conventional blends, which could be calculated from the following formula:

$$V_{POE} = \frac{\rho_B - \rho_{PP}}{\rho_{POE} - \rho_{PP}} \tag{1}$$

where V_{POE} is the volume fraction of POE; ρ_B is the density of the blends; ρ_{PP} and ρ_{POE} represent the densities of neat PP and POE, respectively. The densities of ρ_B, ρ_{PP} and ρ_{POE} were measured through a high precision density tester (MatsuHaku, GH-120M). The blends are coded according to the abbreviation for alternating multilayered blends "A", the number of layers and the volume content of POE. For example, A2-128 represents the 128 layers multilayered blend with 16.21 vol% POE. As for the conventional blends and neat PP, the abbreviation is "C".

Table 1. Sample code, total thickness of the sheets, the average PP and POE layer thickness and the POE volume content

Sample code		Total sheets thickness (μm)	The number of layers	Average POE layers thickness (μm)	Average PP layers thickness (μm)	POE content (vol%)
Conventional blends	C0	1280	—	—	—	0
	C1	1310	—	—	—	6.79
	C2	1320	—	—	—	16.57
Alternating multilayered blends	A1-8	1340	8	23.1	311.2	6.80
	A1-32	1330	32	5.5	77.3	6.91
	A1-128	1250	128	1.3	18.2	6.71
	A2-8	1390	8	57.3	289.4	16.53
	A2-32	1360	32	14.8	70.4	16.98
	A2-128	1225	128	3.4	16.6	16.21

RUSULTS AND DISCUSSION

Phase Morphology

The most distinct difference of the multilayered and conventional blends is that the multilayered blends consist of the alternating PP and POE layers, which can be presented well in Fig. 3. The darker layers in the images belong to the amorphous POE layers, whereas the brighter layers belong to the crystalline PP layers. Moreover, one can observe that the PP and POE layers align alternately vertical to the interfaces and continuously parallel to the extrusion direction. As for the conventional blends (C1 and C2), the addition of POE seems to decrease the sizes of the PP spherulites. Given the unique micro-structure of the multilayered samples can greatly influence the fracture behaviors of the PP/POE system, the corresponding fracture morphologies will be investigated in detail later.

Load-displacement Curves

The *l-d* curves of DENT specimens for PP/POE multilayered and conventional blends with different POE contents are shown in Fig. 4. All the *l-d* curves, which were obtained from the DDENT specimens with different ligament lengths, except for the C2 (POE content 16.57%), present good self-similarity. After the maximum load, a smooth and slow drop in the load occurs, and the ligament begins to yield. After the complete yielding of the ligament, the cracks begin to propagate in a stable manner until the final fracture of the samples. In addition, the maximum load, the displacement to failure, and the area under the curves all increase regularly with increasing ligament length, indicating that the mode of fracture is independent on ligament length. These

behaviors validate the EWF testing and ensure that the cracks propagate under similar stress conditions[38]. As for the C2, after the maximum load, a much slower drop in the load follows by the yielding of the ligament. After the complete yielding of the ligament, the cracks begin to propagate in a stable manner until some particular displacement, and then the cracks propagate in a fast way until the final fracture of the samples. Additionally, for C2, the *l-d* curves, the maximum load and the displacement to failure irregularly increased with increasing the ligament length, moreover, the curves not present any self-similarity, indicating the invalidation of the EWF testing method.

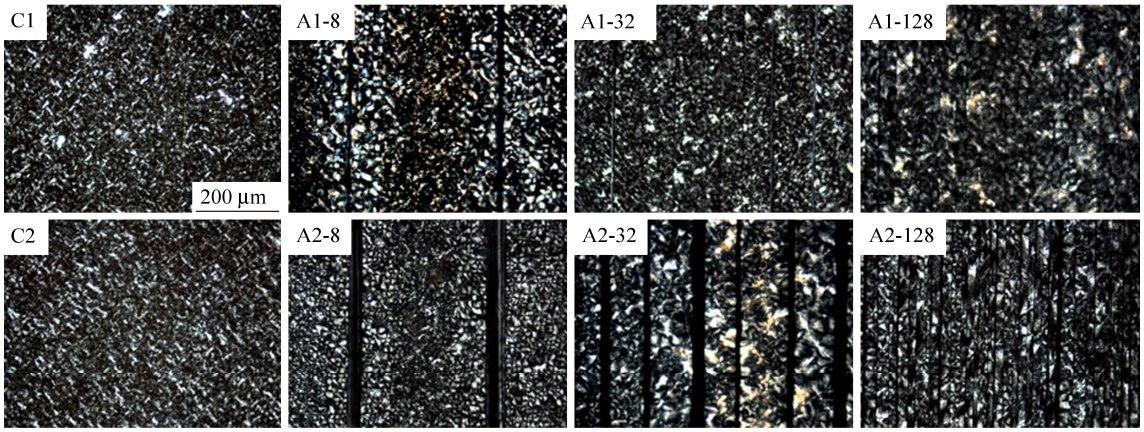


Fig. 3 Polarized optical micrographs of the conventional blends and multilayered blends morphologies (All the scales are the same.)

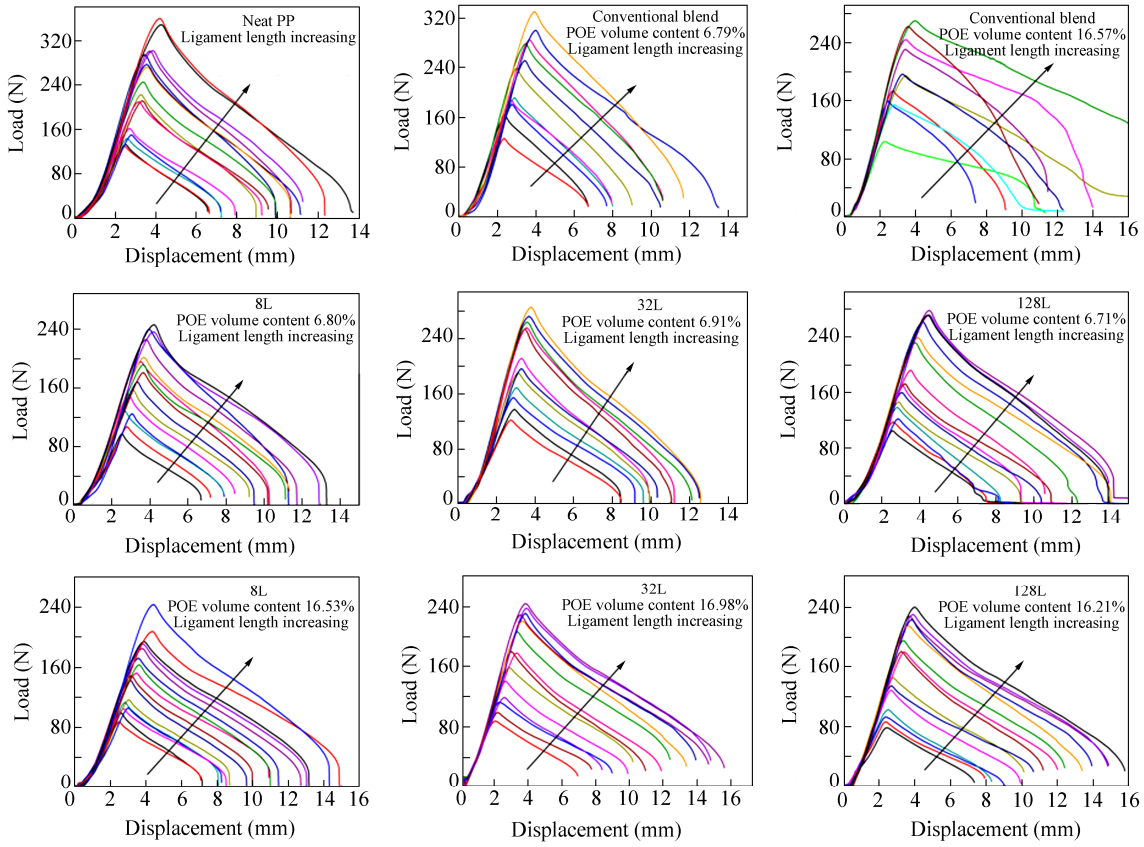


Fig. 4 Load-displacement curves for neat PP, multilayered PP/POE and conventional blends (The POE volume content and the number of layers of the multilayered blends are given in each profile)

Fracture Parameters of the EWF Test

Figure 5 shows that the w_f-l diagrams give good linear relationships for each group. The values of w_e and βw_p, which were obtained from the interception and slope of the straight lines extrapolated to zero ligament length, together with the regression coefficient, are presented in Fig. 6. The linear regression coefficients (R^2) are high than 0.95, showing a good linear correlation. As the Fig. 6(a) shows, the incorporation of POE with a conventional manner increases the w_e value of the blend obviously. Note also that for the high POE content system C2, although the invalidity of EWF testing method, the much slower drop in load after maximum load, is an indicative sign for the improvement of the crack resistance and a much higher w_e value. As for the multilayered blends, the layer number has dramatic effects on their w_e values. In detail, the w_e values of the multilayered blends obviously increase with increasing their layer number. In the case of the same layer number, in particular the 8-layer, one can observe that the w_e values of the multilayered blends with high POE content are abnormally low compared to those with low POE content. Interestingly, the same change trend in the Izod values was also found in our previous work, unlike the conventional blends, the multilayered blends with low POE content have high Izod values compared to those with high POE content[9]. Generally, the introduction of POE into PP often increases the w_e values of PP/POE blends[25, 26]. However, it's nearly no difference in the w_e values of the neat PP (C0) and multilayered blend A1-8, moreover, an obvious drop in the w_e value can be found in the

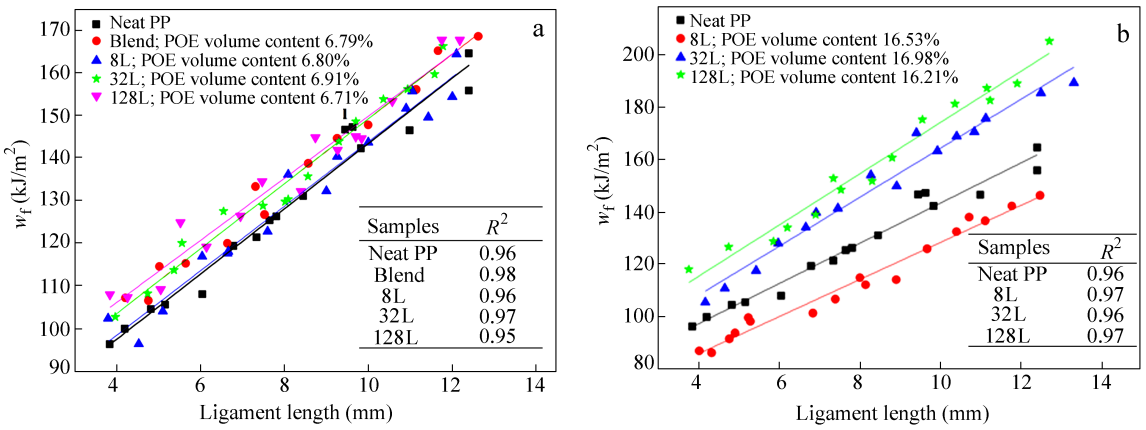


Fig. 5 Specific work of fracture w_f as a function of the ligament length l of the neat PP, alternating multilayered and conventional blends

The spots with different shapes represent the experimental data, while the straight lines are fitting results. ((a), (b) POE volume content is about 6.79% and 16.57%, respectively. R^2: the linear regression coefficients).

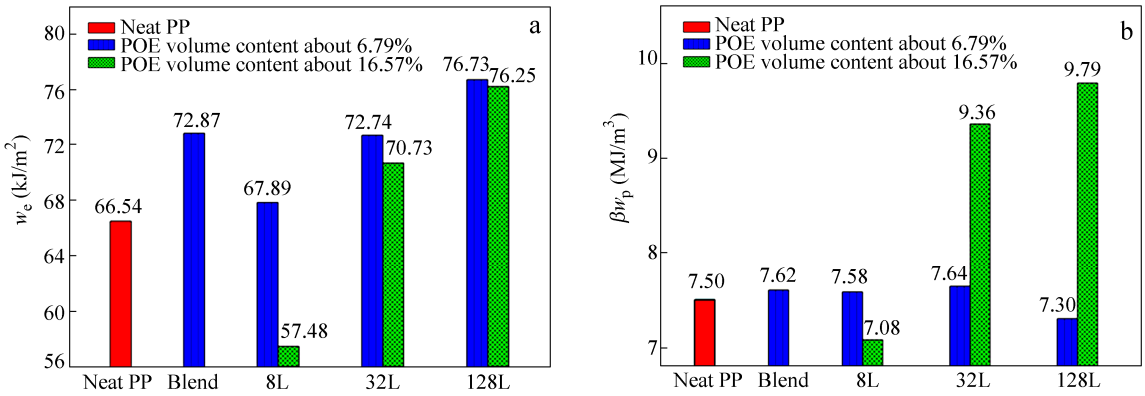


Fig. 6 EWF parameters of the neat PP, conventional blend C1 and the multilayered PP/POE specimens with different layers (The L in the bottom of the diagram is the abbreviation of the layer.)

multilayered blend A2-8. On the basis of the theory of EWF, w_e is the work required to generate new surfaces in inner fracture process zone and relates to its inner fracture surface morphologies, the more new surfaces are created, the higher magnitude of the w_e would be[37, 39].

In order to in-depth understand the variation of the w_e between conventional and multilayered blends, the inner fracture surface morphologies of the samples after EWF tests were observed by SEM. Figure 7 shows the inner fracture surface morphologies of neat PP (C0), conventional blends C1 and C2, and the multilayered samples with different layer numbers. According to the EWF theory, the w_e is related to the inner fracture morphology, the severer of the deformation or the coarser of the inner morphology is, the higher value of the w_e will be. The amounts of micro-thin fibril, which arises from severe matrix plastic deformation, are revealed in the inner fracture region of neat PP (Fig. 7 micrographs C0, c0), and this is consistent with the high w_e value of the neat PP. Compared with the size scales of the micro-thin fibril in the neat PP, much thinner rod-like voids surrounded by the local matrix shear deformation are observed in the micrographs C1 and c1 (Fig. 7), which means the coarser inner fracture morphology. Consequently, the higher w_e value of the conventional blend C1 can be ascribed to its considerable smaller sizes of the long rod-like voids and the surrounding matrix shear yielding. Owing to the POE particles act as the stress concentrate sites, the PP matrix around the POE particles would undergo high spherical stress filed when the blends were suffer from an external stress. Therefore, when the POE content is higher, the distance between two neighboring POE particles is smaller and the adjacent stress field becomes overlap, in such case, beside the deformation of the POE particles and the debonding between the POE particles and PP matrix, the overlap of the adjacent stress fields will initiate the local shear yielding in PP matrix, and subsequently result in the overwhelm deformation of PP matrix as shown in the micrographs C2 and c2 (Fig. 7). Herein, the much slower load drop after maximum load in the load-displacement curves of C2 (Fig. 4) can be ascribed to the efficiency to initial the shear yielding of its PP matrix. As for the multilayered blends, their clear layer structure is well demonstrated in Fig. 3, while after the EWF test, the multilayered structure, especially for the 128-layer multilayered blends, is not easy to be distinguished by the SEM images since the PP layers present long rod-like morphologies. For the multilayered blend A1-8, the size scales of its long rod-like voids are bigger than those of the rod-like voids in blend C1 while comparable to those of the micro-thin fibril in C0, which can explain its comparable w_e with that of the neat PP C0 and lower w_e than that of blend C1. On further increasing the layer number to 128, considerable longer and denser rod-like voids are observed, resulting in the higher w_e value of the A1-128 compared to the C1 and A1-8. On the other hand, for the high POE content A2-8, although the obvious yielding of the PP matrix is formed, the large sizes of its voids indicate the less surface generated during EWF test, leading to its extremely low w_e value. For the A2-128, the morphologies in the inner fracture zone are similar to those of the A1-128, which is consistent with their close w_e values. As for the βw_p, shown in Fig. 6(b), the βw_p values of the A2-128 and A2-32 are obvious higher than those of the A1-128 and A1-32, while the βw_p of the A2-8 is lower than that of the A1-8. As the aforementioned description, the βw_p is not a material constant and depends on the shape of the plastic zone. In order to illustrate the difference of the different βw_p values of the different multilayered blends, two typical shapes of the plastic zone of the multilayered blends are shown in the Fig. 8. Obviously, the plastic zone in the A2-128 is larger than that in A1-128, which is consistent with their βw_p values. Base on the above discussion, we herein attempt to summarize the influences of the POE content and the POE distributing morphology on the EWF parameters of the PP/POE blends. As shown in the Fig. 5(a, b), for the multilayered blends with the same POE content and the same ligament, the w_f values (specific fracture work) of the multilayered blends increase with increasing their layer number. As for the w_e and βw_p (Fig. 6 (a, b)), the w_e values also increase with increasing the layer number. When come to the βw_p, there is no obvious variation for the low POE content multilayered blends, while in the high POE content multilayered blends obvious increasement occurs with increasing their multilayered layer number. As for the low POE content conventional blend C1, obvious increasement for the w_e and slight increasement for the βw_p are observed. Herein, we can conclude that (i) for the multilayered blends with low POE content (A1-8–A1-128), as well as the low POE content conventional blend C1, the increasement of the fracture energy is mainly due to the enhancement of the w_e, in other word, the increasement of the fracture

energy is mainly due to the enhancement of energy that generates the new surfaces; (ii) while for the multilayered blends with high POE content and high layer number, both the enhancements of the w_e and the βw_p lead to the increasement of their fracture energy, in other words, both the energy that consumed to generate the new surfaces and the energy that consumed by the deformation process increase.

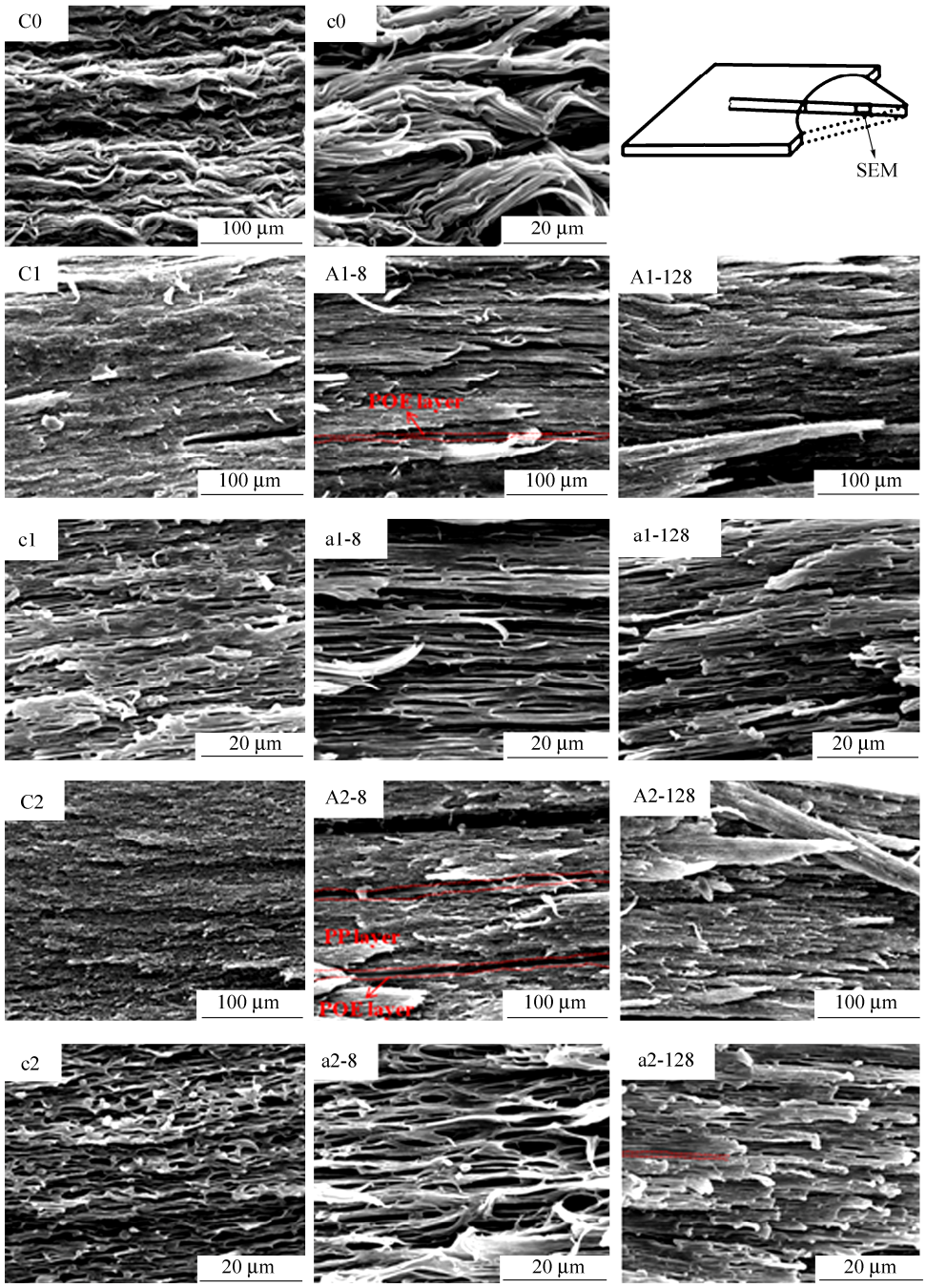


Fig. 7 Fracture surface micrographs of neat PP, conventional and multilayered blends with different magnification after EWF tests

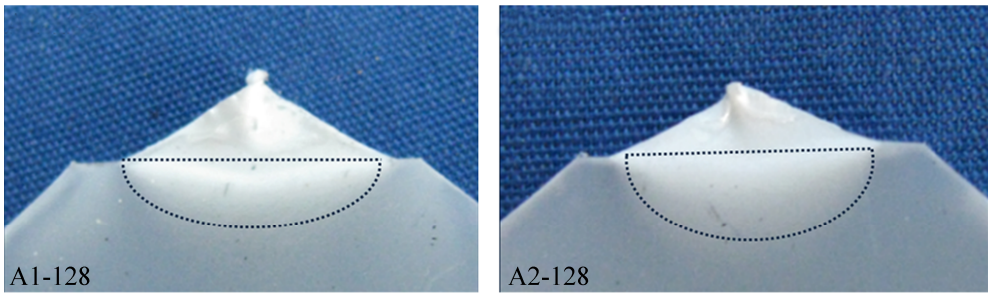


Fig. 8 Photographs showing the plastic zones of the A1-128 and A2-128 with the same geometry for the EWF test

Impact Tensile Tests

Since polymer materials are viscoelastic, their fracture behaviors generally exhibit geometry and strain-rate dependence. In order to further evaluate the toughning behavior of the multilayered blends, besides the quasi-static uniaxial tensile EWF test, the dynamic impact tensile test was also conducted. As shown in Fig. 9, the impact tensile strengths of multilayered blends enhanced obviously with increasing the layer number[9]. For the low POE content system, the impact tensile strengths of alternating multilayered blends A1-128 (781.3 kJ/m^2), A1-32 (442.0 kJ/m^2) and A1-8 (381.8 kJ/m^2) are about 1.8, 1 and 0.86 times that of their conventional blend C1 (443.8 kJ/m^2), respectively. For the high POE content system, the impact tensile strengths of alternating multilayered blends A2-128 (855.6 kJ/m^2), A2-32 (666.2 kJ/m^2), and A2-8 (411.7 kJ/m^2) are about only 1.2, 0.94 and 0.58 times that of their conventional blend C2 (712.0 kJ/m^2), respectively. While the neat PP with different layers presents a stable value about 520 kJ/m^2. Interestingly, compared with C1, A1-8, A1-32 and A2-8, the neat PP exhibits a high impact tensile value. Unlike the EWF test, for the impact tensile test, it's hard to quantitatively distinguish the energy that is consumed to generate new surfaces or that dissipated in the plastic deformation process. However, the total fracture energy can be classified to create the fracture surface and to form the bulk damage beneath the fracture surface. Therefore, inspecting on the fracture surface morphologies and the bulk morphologies is favoring to understand the toughening mechanism. In our previous work, we focused on the low POE system due to its excellent Izod values. However, just for the values of the impact tensile strength, the high POE system presents higher impact tensile values and complicated fracture process. Therefore, the fracture morphologies of the high POE system are investigated here. As shown in Fig. 10, exclusive fracture surface morphologies are observed in A2-128, more information can be revealed through the close-up of the rectangular dashed zones in A2-128 (Figs. 10(a1–a4)). Clear layer structure was found in Figs. 10(a1) and 10(a3), in which the surface of POE layers is very smooth while amounts of shear yielding are found in the PP layers, conversely, the vague layer structure accompanied with some delaminations is observed in Figs. 10(a2) and 10(a4). Most interestingly, an obvious necking region is found in A2-128, resulting in the complicated bulk morphologies beneath the fracture surface (Figs. 10(A1–A6)). Slight delaminations are revealed in the region close to the fracture surface (Figs. 10(A1) and 10(A2)). Obvious delaminations are formed for the warping region in spite of the further distance from the fracture surface (Figs. 10(A3) and (A4)). Moving beyond the neck region leads little effects on the bulk morphology (Figs. 10(A5) and 10(A6)). Necking, the results of the overall yielding and deformation of the materials, is an effective way to dissipate energy. Since the necking region extends to 4000 μm away from the fracture surface in A2-128, which is the key contributor for its high impact tensile strength, besides, the course fracture surface also make important role for its high impact tensile strength. On the other hand, for the A2-8, although the obvious delaminations are found in its fracture surface (Fig. 11(b2)), the necking region is absent, as for its PP layers, rather smooth morphologies with little local shear yielding are observed (Fig. 11(b1)). Besides, the extent of the shear yielding drops with increasing the distance from the fracture surface obviously, which just as shown well with the series of the images (Figs. 11(B1–B3)). Just as the aforementioned description, the necking is an effective way to dissipate energy, therefore, we can own the extremely low impact tensile strength of the A2-8 to the absent of the necking phenomena during impact tensile test. As the above description, the most different fracture behavior of the A2-8

and A2-128 is that the absent of necking in the A2-8. Actually, Ji *et al.*[40] simulated the toughening behavior of a multilayered bio-composite specimen by computer and they concluded that the multilayered structure can redistribute and homogenize stress concentration, what's more, they also observed the high shear yielding regions between the long sides of mineral layers. The shear yielding of the mineral layers is impossible since its high rigidness. However, in the PP/POE multilayered blends, even the "hard" PP layer can deform, and the redistribution and homogenization of the stress concentration may lead to the overall yielding of the PP layers, which finally caused the necking in A2-128. However, according the conclusion of Ji *et al.*[40] and Jäger *et al.*[41], there should be a shear yielding deformation region in the POE layers. While it's difficult to observe the overall yielding of the PP layers due to the thick PP layers in A2-8. Besides, the deformation of the POE would be relaxed due to the high mobility of the POE molecules. We should notice that there is some difference in the architecture between the PP/POE multilayered blends and the multilayered bio-composites, hence, much work should be done in the next step to make more in-depth understanding of the toughening behavior of the PP/POE multilayered blends. As for the neat PP C0 and conventional blend C2, obvious local shear yielding is revealed

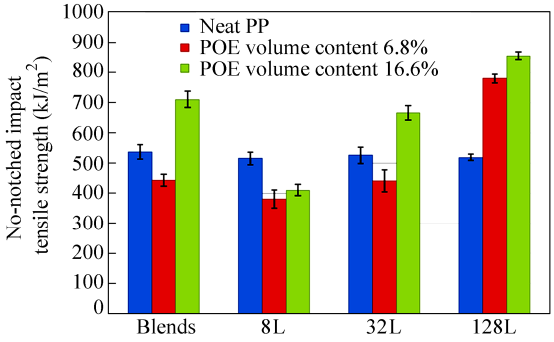


Fig. 9 No-notched impact tensile strength of the neat PP, multilayered and conventional blends with different POE contents (The L is the abbreviation of the layer.)

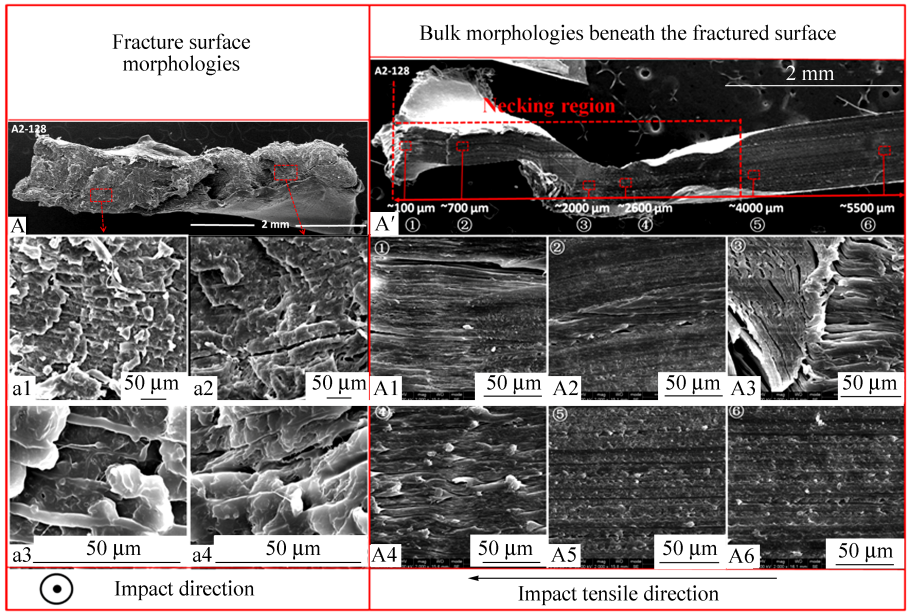


Fig. 10 SEM images of the no-notched impact tensile fracture surface morphologies and the bulk morphologies beneath the fracture surface of the multilayered blend A2-128 at different magnifications: (A1–A6) magnified micrographs taken at the locations as indicated with ①–⑥

in the fracture surface of the C2 (Figs. 12(c1) and 12(c2)) but a rather smooth surface is found in C0 (Figs. 12(a1) and 12(a2)). As for their bulk morphologies, there is an apparent boundary lay between the necking region and the un-necking region (Figs. 12(A2) and 12(C2)). The morphologies before the boundary belong to the necking zone characterized with obvious deformation (Figs. 12(A1) and 12(C1)) while beyond the necking zone the morphologies appear not be affected (Figs. 12(A3) and 12(C3)). Compared with the neat PP C0, the extent of the shear yielding of the conventional blend C2 is much severer than that of the C0 (Figs. 12(C1) and 12(C2)). Besides, as obvious local shear yielding still can be found in the distance of 700 μm, indicating that a bigger necking region in the conventional blend C2. As for their impact tensile strengths, both the obvious shield yielding in the fracture surface and the large necking region of the conventional blend C2 lead to its high impact tensile strength compared to the neat PP C0. As for the fracture morphologies and the bulk morphologies of the low POE content PP/POE blends, complicated morphologies are also observed (not shown in here), which lead to their different impact tensile performance.

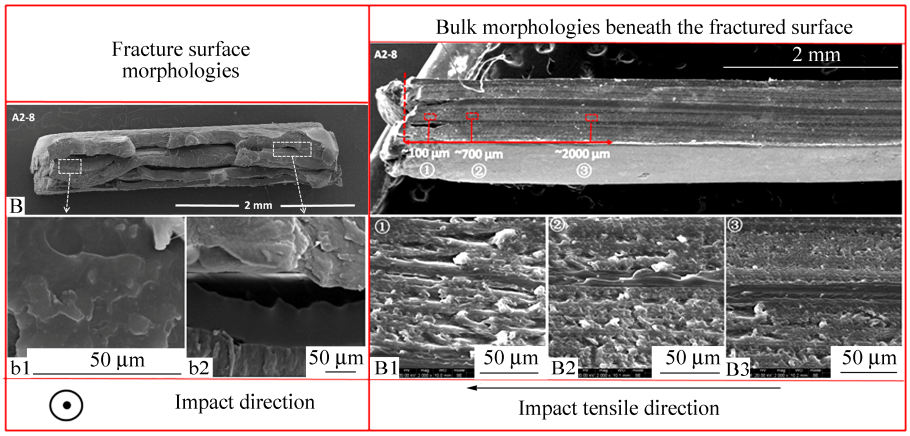


Fig. 11 SEM images of the no-notched impact tensile fracture surface morphologies and the bulk morphologies beneath the fracture surface of the multilayered blend A2-8: (B1–B3) magnified micrographs taken in the locations as indicated with ①–③

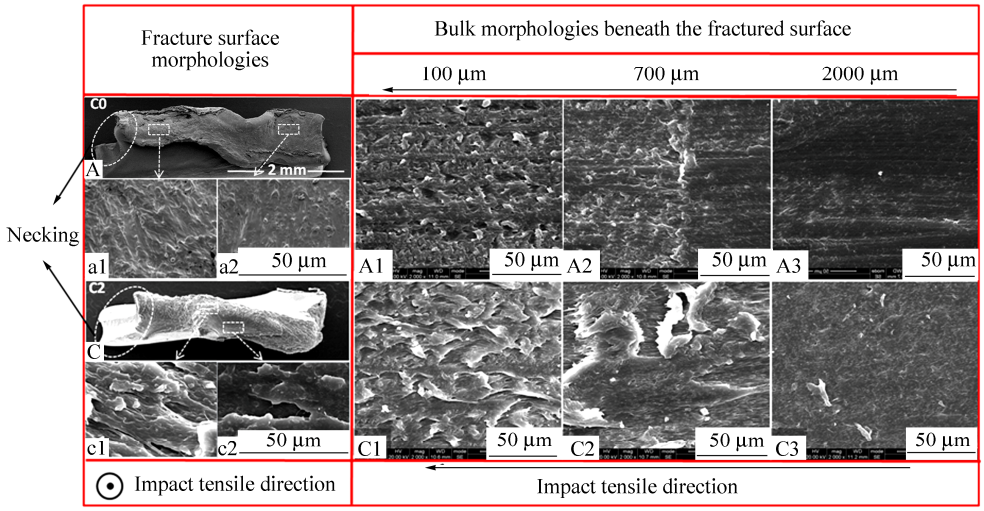


Fig. 12 SEM images of the no-notched impact tensile fracture surface morphologies and the bulk morphologies beneath the fracture surface of the conventional blend C2 and neat PP C0
The subscript 1, 2 and 3 of the A1–A3 and C1–C3 present 100 μm, 700 μm and 2000 μm away from the fracture surface, respectively.

CONCLUSIONS

In this work, two different POE contents (6.79 vol% and 16.57 vol%) multilayered blends and their corresponding conventional blends were successfully fabricated. The EWF and the impact tensile methods have been successfully used to characterize the effects of the different micro-architectures of the POE dispersing phase on the fracture properties of the PP/POE blends. The results show that the layer number has great influences on the w_e values of the multilayered blends, and the w_e values dramatically increase with increasing their layer number. As for the βw_p, there is no obvious variation in the multilayered blends with 6.79% POE content, however, obvious enhancement with increasing the layer number in the 16.57% POE content multilayered blends was observed. Moreover, the impact tensile strength of the multilayered blends also increases with increasing their layer number. Compared with the conventional sea-island structure, the alternating multilayered structure, especially for the system with a lower POE content, is effective to obtain the high toughness materials. Thus, this work may offer some practical clues for toughening PP or other materials with a low elastomer content.

REFERENCES

1 Geng, C., Su, J., Han, S. and Fu, Q., Polymer, 2013, 54(13): 3392
2 Zhang, L., Huang, R., Li, L.B. and Wang, G., J. Appl. Polym. Sci., 2002, 83(9): 1870
3 Zhang, L., Huang, R., Li, L.B., Wang, G. and Zhang, X.L., J. Appl. Polym. Sci., 2002, 86(8): 2085
4 Lee, H., Fasulo, P.D., Rodgers, W.R. and Paul, D.R., Polymer, 2005, 46(25): 11673
5 Wang, J.F., Wang, C.L., Zhang, X.L. and Wu, H., RSC Adv., 2014, 4(39): 20297
6 Currey, J.D., Proc. R. Soc. London. Ser. B., 1977, 196(1125): 443
7 Jackson, A. and Vincent, J.R., Proc. R. Soc. London. Ser. B., 1988, 234(1277): 415
8 Wang, R.Z., Wen, H.B., Cui, F.Z. and Zhang, H.B., J. Mater. Sci., 1995, 30(9): 2299
9 Li, C.H., Yang, S., Wang, J.F., Guo, J.W. and Wu, H., RSC Adv., 2014, 4(98): 55119
10 Bonderer, L.J., Studart, A.R. and Gauckler, L.J., Science, 2008, 319(5866): 1069
11 Lin, T.H., Huang, W.H., Jun, I.K. and Pen, J., J. Colloid Interface Sci., 2010, 344(2): 272
12 Rafael, L., Frédéric, H.L.M., Davi, M.M. and André, R.S., Compos. Sci. Technol., 2012, 72(3): 435
13 Bonderer, L.J., Feldman, K. and Gauckler, L., Compos. Sci. Technol., 2010, 70(13): 1966
14 Bonderer, L.J., Feldman, K. and Gauckler, L., Compos. Sci. Technol., 2010, 70(13): 1958
15 Corni, I., Harvey, T.J., Wharton, J.A., Stokes, K.R., Walsh, F.C. and Wood, R.J.K., Bioinspir. Biomim., 2012, 7(3): 031001
16 Mueller, C.D., Nazarenko, S., Ebeling, T., Schuman, T.L., Hiltner, A. and Baer, E., Polym. Eng. Sci., 1997, 37(2): 355
17 Xu, S.X., Wang, M., Li, J. and Guo, S.Y., Polymer, 2008, 49(22): 4861
18 Chen, B.S., Gao, W.L., Shen, J.B. and Guo. S.Y., Compos. Sci. Technol., 2014, 93: 54
19 Gupta, M., Lin, Y.J., Taneisha, D., David, A.S. and Baer, E., Macromolecules, 2010, 43(9): 4230
20 Tangirala, R., Baer, E., Hiltner, A. and Weder, C., Adv. Funct. Mater., 2004, 14(6): 595
21 Baer, E., Hiltner, A. and Keith, H., Science, 1987, 235(4792): 1015
22 Burt, T.M., Jordan A.M. and Korley, T.J.K., ACS Appl. Mater. Inter., 2012, 4(10): 5155
23 Haderski, D., Sung, K., Hiltner, A. and Baer, E., J. Appl. Polym. Sci., 1994, 52(2): 121
24 Sun, X., Shen, H.W., Xie, B.H. and Yang, M.B., Polymer, 2011, 52(2): 564
25 Wang, L., Xie, B.H., Yang, W., Shen, Y.X. and Yang, M.B., J. Elast. Plast., 2010, 42(2): 101
26 Fu, Z., Dai, W.L., Yu, H.M., Zou, X.X. and Chen, B., J. Mater. Sci., 2011, 46(5): 1272
27 Cotterell, B. and Reddel, J.K., Int. J. Fract., 1977, 13(3): 267
28 Broberg, K.B.J., Mech. Phys. Solids, 1975, 23(3): 215
29 Karger-Kocsisa, J., Bárányb, T. and Moskalac, E.J., Polymer, 2003, 44(19): 5691

30 Karger-kocsis, J. and Bárány, T., Polym. Eng. Sci., 2002, 42(7): 1410
31 Wong, J.S.S., Ferrer-Balas, D., Li, R.K.Y. and Mai, Y.W., Acta Mater., 2003, 51(16): 4929
32 Ganß, M., Staudinger, U., Thunga, M. and Schneider, K., Polymer, 2012, 53(10): 2085
33 Gray, R. "Test protocol for essential work of fracture", Les Diablerets: ESIS TC-4 Group, 1998
34 Arkhireyeva, A. and Hashemi, S., Polymer, 2002, 43(2): 289
35 Martinez, A.B., Segovia, A. and Gamezperez, J., Eng. Fract. Mech., 2010, 77(14): 2654
36 Cotterell, B. and Reddell, J.K., Int. J. Fract., 1977, 13(3): 267
37 Bárány, T. and Czigány, T., Prog. Polym. Sci., 2010, 35(10): 1257
38 Gong, G., Xie, B.H., Yang, W., Li, Z.M. and Yang, M.B., Polym. Test., 2005, 24(4): 410
39 Martinez, A.B., Gamezperez, J., Sanchezsoto, M., Velasco, J.I. and Maspoch, M.L., Eng. Fail. Anal., 2009, 16(8): 2604
40 Ji, B. and Gao, H.J., Mater. Sci. Eng., 2004, 366(1): 96
41 Jager, I. and Fratzl, P., Biophys. J., 2004, 79(4): 1737